AD-A168 599 A CONTINUUM THEORY OF CRACK SHIELDING IN CERAMICS(U) 1/1
BROWN UNIV PROVIDENCE RI DIV OF ENGINEERING M ORTIZ
22 MAY 86 N00014-85-K-0720

UNCLASSIFIED F/G 11/2 NL

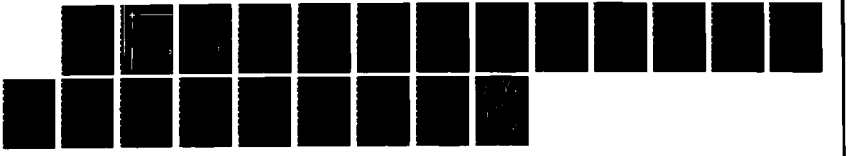

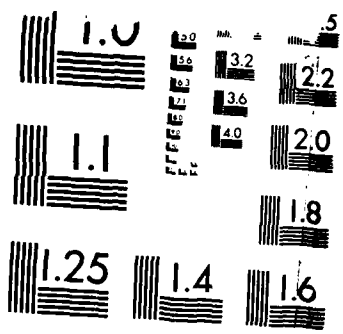

Brown University
DIVISION OF ENGINEERING
PROVIDENCE, R.I. 02912

A Continuum Theory of Crack Shielding in Ceramics

by

M. Ortiz
Division of Engineering
Brown University
Providence, RI 02912

A Continuum Theory of Crack Shielding in Ceramics

by

M. Ortiz
Division of Engineering
Brown University
Providence, RI 02912

Contract No.: N00014-85-K-0720

May 22, 1986

A Continuum Theory of Crack Shielding in Ceramics

M. Ortiz

Division of Engineering, Brown University, RI 02912, USA

Abstract - A phenomenological constitutive model is proposed which aims at describing the overall effect of microfracture in ceramics. Based on this model, the asymptotic stress, strain and displacement fields at the tip of a stationary macroscopic crack are determined in closed form. The near-tip stress-intensity factor is computed and observed to be significantly smaller than the applied stress-intensity factor even for moderate amounts of damage.

1 Introduction

Certain classes of ceramics are known to undergo extensive microcracking confined to a process zone surrounding macrocrack tips [1-3]. Under these conditions, the processes at the crack tip are screened from the remote loads by the intervening microcracks and a fracture toughness enhancement results [4]. Microcracks develop at grain boundary facets mainly as a result of residual stresses generated during cooling and of applied tensile stresses [5]. The net effect of the microcracks is to render the material more compliant. Under increasing loads, the microcracks already present in the material remain confined to their respective facets and their size essentially unaltered. Thus, further elastic degradation comes about as a result of increasing microcrack density and not microcrack growth. Eventually, the number of available nucleation sites which are favorably oriented with respect to the applied tensile loads is exhausted and a saturation stage is reached in which the material does not undergo further damage.

A first attempt at quantifying the crack shielding effect [6] has relied on computer simulation. However, an analytical treatment of the problem has proven elusive in part due to lack of adequate material characterization. In this study it is assumed that the length scale over which the singular fields dominate is large compared with the characteristic microcrack size and the

mean distance between the microcracks so that an asymptotic analysis can be based on the effective overall properties of the continuum. Ideally, one would like to have a description of the effective behavior based on micromechanics and a detailed knowledge of its dependence on relevant micromechanical parameters such as grain size. However, this entails the determination of the aggregate effect of dense populations of strongly interacting microcracks, possibly with preferred orientations, distributed over a three-dimensional heterogeneous elastic medium. Even under strong simplifying assumptions, this problem poses considerable difficulties [7,8]. Thus, to make progress one has to resort to phenomenological models. In Section 2, one such model is proposed which aims at describing the effective behavior of a material undergoing progressive distributed damage and exhibiting a saturation stage. The possibility of a strong damage-induced elastic anisotropy is taken into consideration. Some of the ideas involved have been taken from constitutive models proposed for other progressively fracturing materials such as concrete [9].

It Section 3 the near-tip singular fields for a stationary crack are determined in closed form. Then, Rice's J-integral [10] is used to relate the stress-intensity factor at the crack tip to the amplitude of the remote K-field. It is found that small amounts of damage can result in a substantial reduction of the stress-intensity factor and thereby bring about a toughening of the material. This situation is in sharp contrast to transformation toughening which only comes into effect for a growing crack [11].

2 Effective Constitutive Behavior of Progressively Fracturing Materials

A phenomenological constitutive model is presented below which aims at describing the overall effect of microfracture in ceramics. In this work, processes resulting in permanent strains as well as rate effects are neglected. The model is predicated upon the following assumptions. Stresses and strains are assumed to be linearly related according to

$$\epsilon_{ij} = C_{ijkl}\sigma_{kl} \tag{1}$$

where the elastic compliances C_{ijkl} are regarded as internal variables which evolve as a result of damage processes taking place at a microstructural level. A threshold is postulated below which no further damage can occur. For the class of materials under consideration, the onset

of damage is assumed to occur when the maximum tensile stress σ_1 reaches a critical value $\sigma_c \geq 0$, i. e.

$$\phi(\boldsymbol{\sigma}, \sigma_c) \equiv \sigma_1 - \sigma_c = 0 \tag{2}$$

The direction of incremental damage is given by a damage rule

$$\dot{C}_{ijkl} = \dot{\lambda} n_i n_j n_k n_l \tag{3}$$

where $\mathbf{n}$, $\sqrt{n_i n_i} = 1$, is the direction of maximum tensile stress and the multiplier λ can be regarded as an effective added flexibility due to damage. Implicit in (3) is the assumption that the newly nucleated microcracks tend to be preferentially oriented normal to the direction of maximum tensile stress and thus most loss of stiffness occurs in that direction. Similar ideas were used in [14] to estimate the macroscopic steady creep-rate of a material exhibiting power-law creep and simultaneously undergoing creep-constrained grain boundary cavitation.

The evolution of the critical stress σ_c is assumed to be governed by a damage rule of the type

$$\dot{\sigma}_c = h(\sigma_c)\dot{\lambda} \tag{4}$$

for some modulus $h(\sigma_c)$. In this simple model the dependence of h on σ_c can be determined from the uniaxial tension stress-strain curve alone. Finally, the damage and loading-unloading criteria can be expressed in Kuhn-Tucker form as the requirement that the constraints

$$\phi \leq 0, \qquad \dot{\lambda} \geq 0, \qquad \phi\dot{\lambda} = 0 \tag{5}$$

be simultaneously satisfied at all times.

It is interesting to note that the above constitutive model shares a common structure with other rate-independent theories such as classical plasticity. In this latter case, a principal objective of the theory is to predict the evolution of the plastic strains while in the case at hand interest is focused on the evolution of the effective elastic moduli. In spite of these similarities, certain aspects of the behavior of materials undergoing microcracking do not have

a counterpart in plasticity. The effect of closure of microcracks under load reversal falls within that category. By this mechanism microcracks can become inactive and cease to contribute to the flexibility of the material. Consideration of this effect requires to add further structure to the model. Microcrack closure can be modelled within a phenomenological theory as a unilateral constraint which requires that the deformation contributed by the microcracks be always tensile in all directions [9]. In the present study attention is confined to monotonic loading processes for which microcrack closure is of no concern.

For the purpose of the asymptotic analysis that follows it proves more convenient to employ a deformation type constitutive theory rather than the incremental model introduced above. A deformation theory of damage can be readily obtained by integrating the incremental constitutive equations along proportional stress paths. This results in the following stress-strain relation

$$\epsilon_{ij} = \Big(C^{o}_{ijkl} + \lambda(\sigma_1) n_i n_j n_k n_l \Big) \sigma_{kl} \tag{6}$$

where C^{o}_{ijkl} are the isotropic elastic moduli of the uncracked material, $\mathbf{n}$ is the direction of maximum tensile stress and the function $\lambda(\sigma_1)$ can be determined directly from the uniaxial tension test. A typical uniaxial tension stress-strain curve is shown in Fig. 1, [5]. It is seen that the material initially exhibits an elastic domain after which damage starts to accumulate. Eventually, a saturation stage is reached wherein no further damage takes places. In this saturation stage eq. (6) simplifies to

$$\epsilon_{ij} = \Big(C^{o}_{ijkl} + \lambda_s n_i n_j n_k n_l \Big) \sigma_{kl} = C^{o}_{ijkl} \sigma_{kl} + \lambda_s \sigma_1 n_i n_j \tag{7}$$

where λ_s is a constant of value

$$\lambda_s = \frac{1}{E_s} - \frac{1}{E_o} \tag{8}$$

Here, E_o is the initial Young's modulus of the material and E_s is the slope of the uniaxial tension stress-strain curve in the saturation range.

The stress-strain relation (6) has a hyperelastic structure

$$\epsilon_{ij} = \frac{\partial \chi(\boldsymbol{\sigma})}{\partial \sigma_{ij}} \tag{9}$$

where the complementary energy potential $\chi(\boldsymbol{\sigma})$ takes the form

$$\chi(\boldsymbol{\sigma}) = \frac{1}{2} C'_{ijkl} \sigma_{ij} \sigma_{kl} + f(\sigma_1) \tag{10}$$

The functions $f(\sigma_1)$ and $\lambda(\sigma_1)$ are related by $f' = \lambda$. In the saturation stage eq. (6) reduces to (7) and $f(\sigma_1)$ to $\lambda_s \sigma_1^2/2$, which renders the complementary energy potential (10) a homogeneous function of degree two of the stress tensor. Therefore, the strain energy potential $W(\boldsymbol{\epsilon})$ is also a homogeneous function of degree two and satisfies the identity

$$W(\boldsymbol{\epsilon}) = \chi(\boldsymbol{\sigma}) = \frac{1}{2} \sigma_{ij} \epsilon_{ij}, \qquad when \quad \epsilon_{ij} = \frac{\partial \chi(\boldsymbol{\sigma})}{\partial \sigma_{ij}} \tag{11}$$

i. e., the strain and complementary energy potentials take the same numerical value when evaluated at stresses and strains which satisfy the stress-strain relations (9).

3 Asymptotic Fields for a Stationary Crack

Throughout this work it is assumed that the region around the crack tip to which microcracking is confined is small compared with the length of the crack but orders of magnitude larger than the characteristic size of the microcracks and their mean separation. Under the first condition an asymptotic problem can be formulated for a semi-infinite crack as shown in Fig. 2. The second condition is needed for the constitutive model presented above to apply. In this paper attention is confined to plane strain conditions and Mode I loading, i. e., applied loads which result in stress fields which are symmetric with respect to the plane of the crack.

Three well-differentiated regions surrounding the crack tip can be identified, Fig. 2. In the innermost region the strains are large enough so that the material can be assumed to be in the saturation stage. On the other hand, at points far away from the crack tip the material behavior is linear isotropic elastic and the state of stress is given by [10]

$$\sigma_{ij}(r, \theta) = \frac{K_\infty}{\sqrt{2\pi r}} \tilde{\sigma}^o_{ij}(\theta) \tag{12}$$

where K_∞ is the remote stress-intensity factor and the universal angular distributions $\tilde{\sigma}^o_{ij}(\theta)$ for a linear isotropic elastic material are given by [10]

$$\left\{ \begin{array}{c} \tilde{\sigma}^{o}_{rr}(\theta) \\ \tilde{\sigma}^{o}_{\theta\theta}(\theta) \\ \tilde{\sigma}^{o}_{r\theta}(\theta) \end{array} \right\} = \left\{ \begin{array}{c} (5/4)cos(\theta/2) - (1/4)cos(3\theta/2) \\ (3/4)cos(\theta/2) + (1/4)cos(3\theta/2) \\ (1/4)sin(\theta/2) + (1/4)sin(3\theta/2) \end{array} \right\} \tag{13}$$

The value of K_∞ depends upon the particular geometry of the cracked specimen and represents the influence of the applied loading. In between the inner and outer fields lies a transition zone in which the material is partially saturated.

The behavior of the material surrounding the crak tip is assumed to be described by the stress-strain law (7). Since these relations derive from a complementary energy potential which is homogeneous of degree two, a classical argument [10] shows that the leading term in the asymptotic expansion of the stress field has to be of the form

$$\sigma_{ij}(r,\theta) = \frac{K_t}{\sqrt{2\pi r}} \tilde{\sigma}_{ij}(\theta) \tag{14}$$

where K_t is the local stress-intensity factor of the near-tip fields and the angular distributions $\tilde{\sigma}_{ij}(\theta)$ are to be determined. In general K_t is different from K_∞ because the crack tip is shielded from the remote loads by the intervening microcracks. Assuming that crack growth is controlled by the value of K_t it becomes of primary interest to determine the relation between K_t and K_∞.

In view of the fact that the constitutive behavior of the material surrounding the crack tip is nonlinear and strongly anisotropic one would expect singular stress fields which substantially depart from the linear isotropic solution. It is shown next that this is not the case. In fact, the linear isotropic stress field provides the exact asymptotic solution of the problem, i. e.

$$\tilde{\sigma}_{ij}(\theta) = \tilde{\sigma}^{o}_{ij}(\theta) \tag{15}$$

Under certain circumstances, a similar situation is encountered in materials exhibiting linear creep and grain boundary cavitation [14]. On the basis of this observation, Hutchinson [14] anticipated the result stated above, namely, that constitutive relation (7) implies the same angular distribution of stresses as in the linear elastic solution.

To prove eq. (15) we start by noting that the stress field (14), (15) satisfies equilibrium and traction-free boundary conditions on the crack faces. Thus, it only remains to be shown that the corresponding strains satisfy compatibility. With reference to Fig. 2, the direction of maximum tensile stress is computed to be

$$\mathbf{n} = (cos\alpha,\ sin\alpha), \qquad \alpha = \begin{cases} \pi/4 - \theta/4, & 0 < \theta \leq \pi; \\ -\pi/4 - \theta/4, & -\pi \leq \theta < 0; \end{cases} \tag{16}$$

Thus, the angle α made by $\mathbf{n}$ and the radial direction varies linearly with the polar angle θ from a value of $\alpha = 45°$ at $\theta = 0^+$ to $\alpha = 0°$ on the crack face $\theta = \pi$. The vector $\mathbf{n}$ can be regarded as giving an indication of the preferred orientation of the microcracks. In this light, it is interesting to note that for $\theta = 0$ one has $\tilde{\sigma}_{rr} = \tilde{\sigma}_{\theta\theta}$ and $\tilde{\sigma}_{r\theta} = 0$. This would appear to render α indeterminate on the plane of the crack. However, this indeterminacy can be resolved by computing the limiting values of α as the plane $\theta = 0$ is approached from above and below. This operation yields two values of $\alpha = \pm 45°$, respectively. Thus, the model predicts two families of perpendicular microcracks at $\theta = 0$ symmetrically distributed with respect to the plane of the crack.

Substituting (16) into (6) the asymptotic strain field is computed to be

$$\begin{Bmatrix} \epsilon_{rr}(r,\theta) \\ \epsilon_{\theta\theta}(r,\theta) \\ \gamma_{r\theta}(r,\theta) \end{Bmatrix} = \frac{K_t}{\sqrt{2\pi r}} \frac{1}{2G_o} \begin{Bmatrix} (5/4 - 2\nu_o)cos(\theta/2) - (1/4)cos(3\theta/2) \\ (3/4 - 2\nu_o)cos(\theta/2) + (1/4)cos(3\theta/2) \\ (1/2)sin(\theta/2) + (1/2)sin(3\theta/2) \end{Bmatrix} + \frac{K_t}{\sqrt{2\pi r}} \lambda_* \left(cos\frac{\theta}{2} + \frac{1}{2} sin\theta \right) \begin{Bmatrix} (1 + sin(\theta/2))/2 \\ (1 - sin(\theta/2))/2 \\ cos(\theta/2) \end{Bmatrix}, \qquad 0 < \theta \leq \pi \tag{17}$$

where E_o, ν_o and $G_o = E_o/2(1+\nu_o)$ are the initial Young's modulus, Poisson's ratio and shear modulus of the uncracked material. It is noted that the first term is the isotropic linear elastic solution corresponding to a stress-intensity factor K_t. The second term respresents the effect of damage and vanishes identically for $\lambda_* = 0$, i. e., $E_* = E_o$. The strains in the lower half plane $-\pi \leq \theta < 0$ are obtained from the symmetry conditions

$$\epsilon_{rr}(r,-\theta) = \epsilon_{rr}(r,\theta), \qquad \epsilon_{\theta\theta}(r,-\theta) = \epsilon_{\theta\theta}(r,\theta), \qquad \gamma_{r\theta}(r,-\theta) = -\gamma_{r\theta}(r,\theta) \tag{18}$$

The computed angular distributions of the strain components are shown in Fig. 3 as a function of the material parameters involved. A noteworthy feature of the solution is that the shearing strain $\gamma_{r\theta}$ exhibits a jump accross the plane of the crack.

Lengthy but straightforward algebra shows that the strain field (17) identically satisfies

the compatibility equation. Hence, eqs. (14), (15) do indeed provide a closed form asymptotic solution of the problem. The displacement field can be computed from the strain-displacement relations to obtain

$$\left\{ \begin{array}{c} u_r(r,\theta) \\ u_\theta(r,\theta) \end{array} \right\} = \frac{K_t}{4G_o}\sqrt{\frac{r}{2\pi}} \left\{ \begin{array}{c} (2\kappa_o - 1)cos(\theta/2) - cos(3\theta/2) \\ -(2\kappa_o + 1)sin(\theta/2) + sin(3\theta/2) \end{array} \right\} + K_t\lambda_e\sqrt{\frac{r}{2\pi}} \left\{ \begin{array}{c} \left(cos(\theta/2) + (1/2)sin\theta\right)\left(1 + sin(\theta/2)\right) \\ cos\theta - sin(\theta/2) - sin^3(\theta/2) - 1 \end{array} \right\}, \qquad 0 < \theta \leq \pi \tag{19}$$

where $\kappa_o = 3 - 4\nu_o$. The displacements in the lower half plane follow from the symmetry conditions

$$u_r(r,-\theta) = u_r(r,\theta), \qquad u_\theta(r,-\theta) = -u_\theta(r,\theta) \tag{20}$$

Of particular interest is the crack opening profile

$$\delta(r) = -u_\theta(r,\pi) + u_\theta(r,-\pi) = 8K_t\left(\frac{1-\nu_o^2}{E_o} + \lambda_e\right)\sqrt{\frac{r}{2\pi}} \tag{21}$$

As can be seen, the opening profile is parabolic as in the linear elastic solution.

The asymptotic analysis presented above has been based on the deformation theory of damage given in Section 2. However, since the stress field about the crack tip is identical to the stress field in the outer undamaged region except for an amplitude factor it can be concluded that the stress paths at all material points are nearly proportional and the solution given above is consistent with the incremental constitutive model as well. A similar situation was encountered by Hutchinson [12] and Rice and Rosengren [13] who based their analysis on a deformation theory of plasticity to find a posteriori that their solution satisfies the incremental constitutive equations as well.

4 Crack Tip Stress-Intensity Factor: Application of the J-Integral

To have a complete asymptotic solution of the problem under consideration is remains to determine the value of the crack tip stress-intensity factor K_t as a function of the amplitude K_∞ of the applied K-field. This relation follows simply from an application of the J-integral of Rice [10]. It has been shown above that under monotonic loading the stress path at all points is nearly proportional and the response of the material is indistinguishable from that of

a small strain, nonlinear elastic solid with complementary energy potential (10). Under these conditions, the formalism of the J-integral applies. Let us recall that

$$J = \int_\Gamma [W(\epsilon) m_1 - \sigma_{ij} m_j u_{i,1}] ds \tag{22}$$

Here, $\mathbf{m}$ signifies the outer normal to the contour Γ encircling the crack tip. If the contour in chosen to lie entirely within the remote field J reduces to the classical expression

$$J_\infty = \frac{1-\nu_o^2}{E_o} K_\infty^2 \tag{23}$$

For a contour shrunk down to the crack tip (22) can be evaluated from eqs. (14), (15) and (19). For the particular material model under consideration the strain and complementary energy potentials coincide in numerical value and $W(\epsilon)$ in (22) can be replaced by $\chi(\sigma)$ as computed from (7), (14) and (15). A lengthy but straightforward computation yields

$$J_t = \frac{1-\nu_o^2}{E_o} K_t^2 + \beta \lambda_s K_t^2 \tag{24}$$

where the numerical constant β takes the value $\beta = 1.0942$. The path-independence of J necessitates

$$J_t = J_\infty \tag{25}$$

from where one finds

$$\frac{K_t}{K_\infty} = \frac{1}{\sqrt{1 + \frac{\beta}{1-\nu_o^2}\left(E_o/E_s - 1\right)}} \tag{26}$$

The dependence of K_t/K_∞ on E_o/E_s is shown in Fig. 4. A substantial reduction in K is observed even for moderate deviations from elastic behavior.

5 Discussion

The analysis presented above has been based on a model of damage in which permanent strains and rate effects are assumed to be negligible. The model incorporates some of the complexities that are encountered in most progressively fracturing materials such as a strong

damage-induced elastic anisotropy. However, the constitutive framework is simple enough that a closed form analytical solution for the asymptotic problem can be obtained.

The computed results are indicative of a significant reduction in the crack tip stress-intensity factor from the remote K. Unfortunately, the net toughness enhancement cannot be expected to be as substantial as Fig. 4 would tend to suggest due to the fact that the microcracks created ahead of the main crack degrade the crack extension resistance of the material [4]. The main microstructural mechanism underlying this latter effect is microcrack coalescence, a process which is poorly understood at present. Thus, it would appear that a detailed understanding of the toughness properties of ceramics will inevitably require further experimental and analytical research.

Acknowledgements - The author is indebted to helpful and stimulating conversations with C. F. Shih and J. W. Hutchinson. The support of the Office of Naval Research through grant N00014-85-K-0720 is gratefully acknowledged.

References

1. Hoagland, R. G., Hahn, G. T., and Rosenfield, A. R., "Influence of Microstructure on the Fracture Propagation in Rock," *Roc. Mech.*, Vol. 5, 1973, pp. 77-106.
2. Claussen, N., "Fracture Toughness of Al_2O_3 with an Unstabilized ZrO_2 Dispersed Phase," *J. Am. Ceram. Soc.*, Vol. 59, 1976, pp. 49-51.
3. Wu, C. C., Freiman, S. W., Rice, R. W., and Mecholsky, J. J., "Microstructural Aspects of Crack Propagation in Ceramics," *J. Mater. Sci.*, Vol. 13, 1978, pp. 2659-2670.
4. Evans, A. G., "Aspects of the Reliability of Ceramics," in *Defect Properties and Processing of High-Technology Monmetallic Materials*, Crawford, J. H., Chen, Y., and Sibley, W. A., eds., pp. 63-80, North-Holland, 1984.
5. Fu, Y., "Mechanics of Microcrack Toughening in Ceramics," Doctoral Dissertation, University of California at Berkeley, 1983.
6. Hoagland, R. G., and Embury, J. D., "A Treatment of Inelastic Deformation around a Crack Tip Due to Microcracking, *J. Am. Ceram. Soc.*, Vol. 63, 1980, pp. 404-410.
7. Horii, H., and Nemat-Nasser, S., "Overall Moduli of Solids with Microcracks: Load-Induced Anisotropy," *J. Mech. Phys. Solids*, Vol. 31, 1983, pp. 155-171.

8. Kachanov, M., "A Simple Technique of Stress Analysis in Elastic Solids with Many Cracks, *Int. J. Fracture*, Vol. 28, 1985, pp. 11-19.

9. Ortiz, M., "A Constitutive Theory for the Inelastic Behavior of Concrete," *Mechanics of Materials*, Vol. 4, 1985, pp. 67-93.

10. Rice, J. R., "Mathematical Analysis in the Mechanics of Fracture," in *Fracture*, Liebowitz, H., ed., Vol. 2, pp. 191-311, Academic Press, 1968.

11. Budiansky, B., Hutchinson, J. W., and Lambropoulos, J. C., "Continuum Theory of Dilatant Transformation Toughening in Ceramics," *Int. J. Solids Structures*, Vol. 19, 1983, pp. 337-355.

12. Hutchinson, J. W., "Singular Behavior at the End of a Tensile Crack in a Hardening Material," *J. Mech. Phys. Solids*, Vol. 16, 1968, pp. 13-31.

13. Rice, J. R., and Rosengren, G. F., "Plane Strain Deformation near a Crack Tip in a Power Law Hardening Material," *J. Mech. Phys. Solids*, Vol. 16, 1968, pp. 1-12.

14. Hutchinson, J. W., "Constitutive Behavior and Crack Tip Fields for Materials Undergoing Creep-Constrained Grain Boundary Cavitation," *Acta Metall.*, Vol. 31, No. 7, 1983, pp. 1079-1088.

Figure Captions

Fig. 1. Uniaxial tension stress-strain curve showing an initial elastic range and a saturation stage.

Fig. 2. Small scale microcracking problem for stationary crack.

Fig. 3. Angular variations of the near-tip strain field ($\nu_o = 0.25$).

Fig. 4. Near-tip stress-intensity factor as a function of the extent of elastic degradation ($\nu_o = 0.25$).

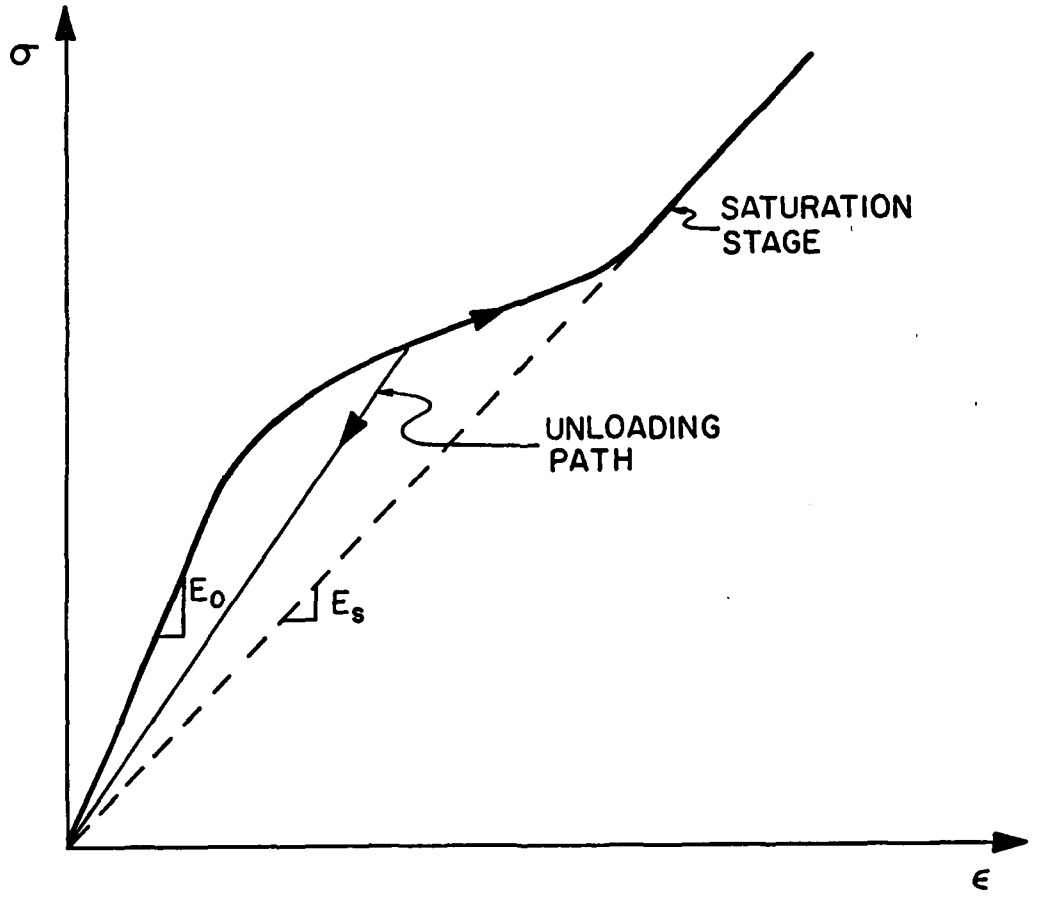

FIG. 1

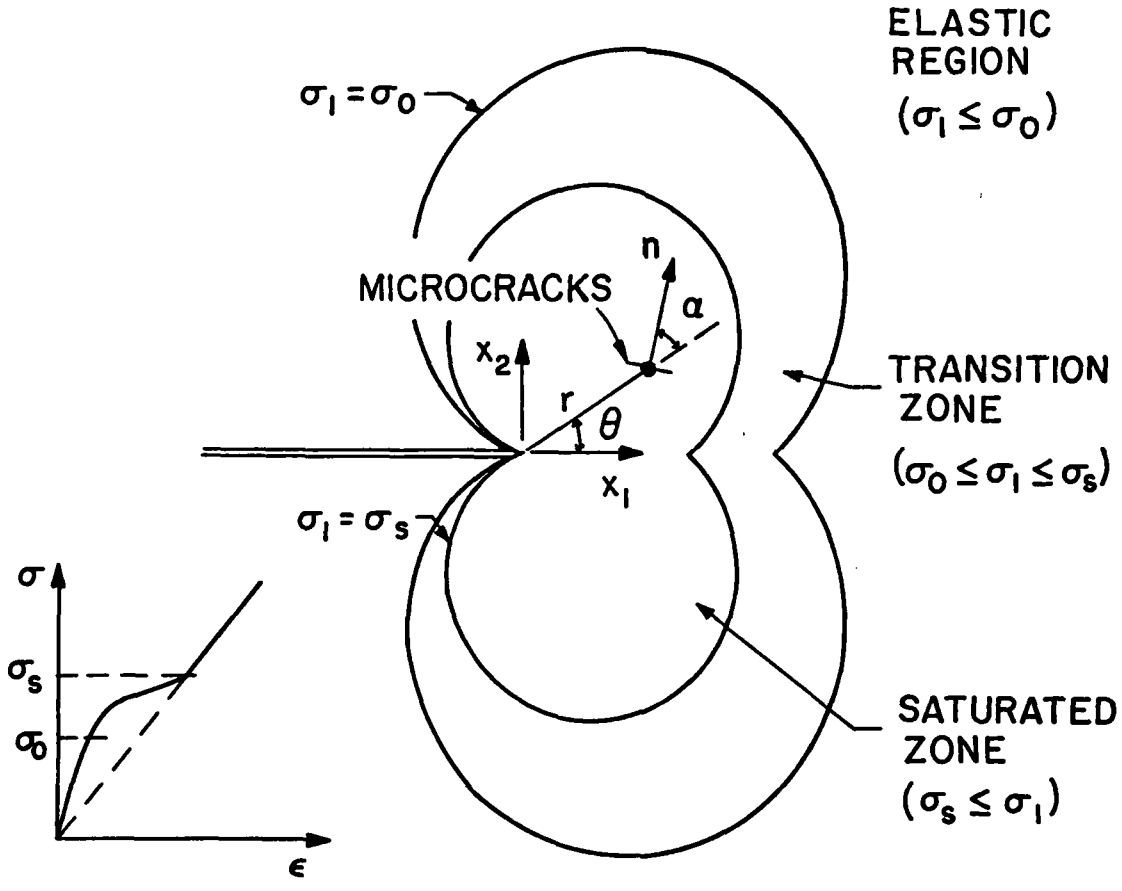
ELASTIC
REGION
$(\sigma_1 \leq \sigma_0)$
$\sigma_1 = \sigma_0$
MICROCRACKS
n
α
x_2
r
θ
x_1
TRANSITION
ZONE
$(\sigma_0 \leq \sigma_1 \leq \sigma_s)$
$\sigma_1 = \sigma_s$
SATURATED
ZONE
$(\sigma_s \leq \sigma_1)$
σ
σ_s
σ_0
ϵ

FIG. 2

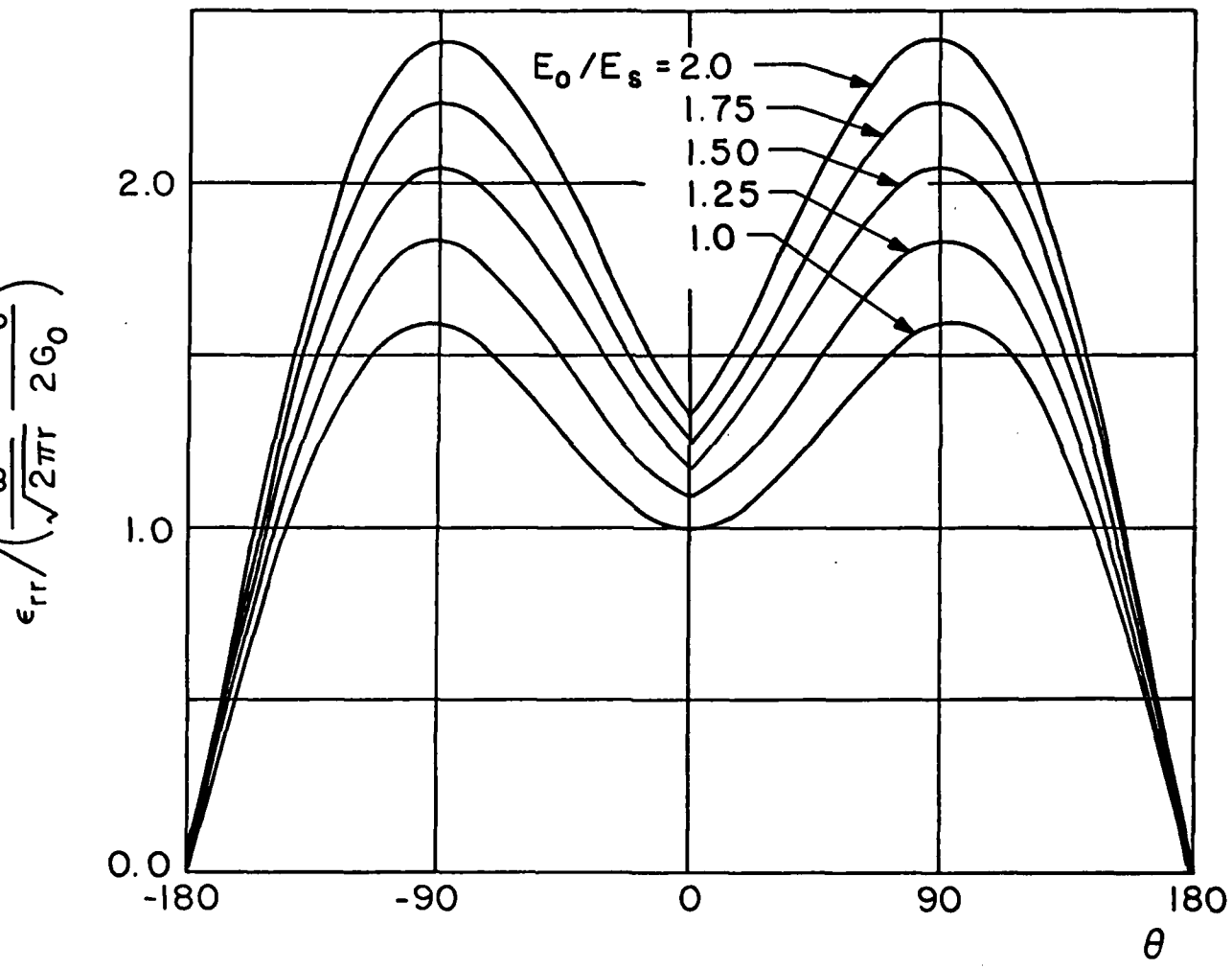
$E_0/E_s = 2.0$
1.75
1.50
1.25
1.0
2.0
1.0
0.0
-180
-90
0
90
180
θ
$\epsilon_{rr} / \left(\frac{K_\infty}{\sqrt{2\pi r}} \frac{1-2\nu_0}{2G_0} \right)$

FIG. 3a

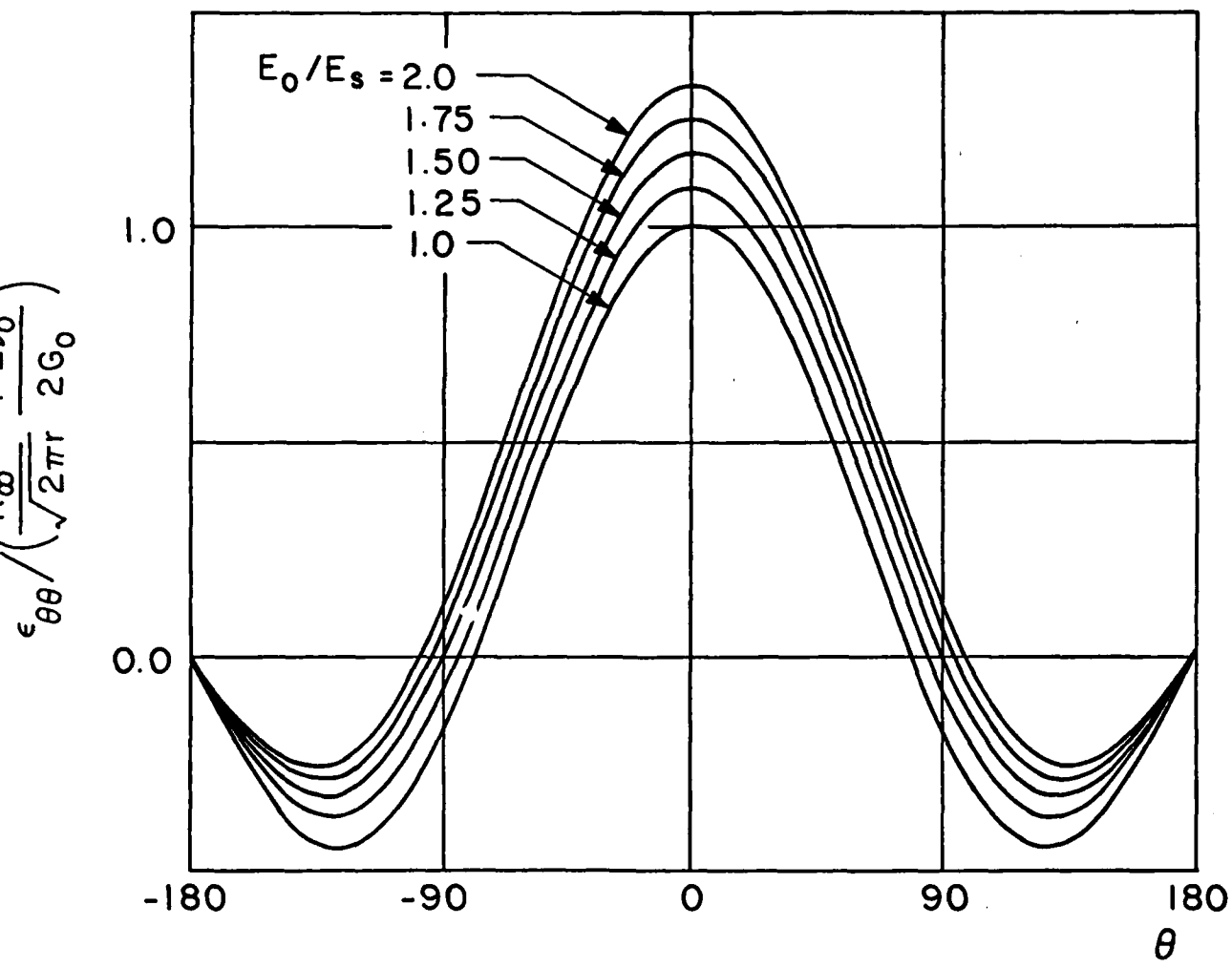
$E_0/E_s = 2.0$
1.75
1.50
1.25
1.0
1.0
0.0
$\epsilon_{\theta\theta}/\left(\frac{K_\infty}{\sqrt{2\pi r}}\frac{1-2\nu_0}{2G_0}\right)$
-180
-90
0
90
180
θ

FIG. 3b

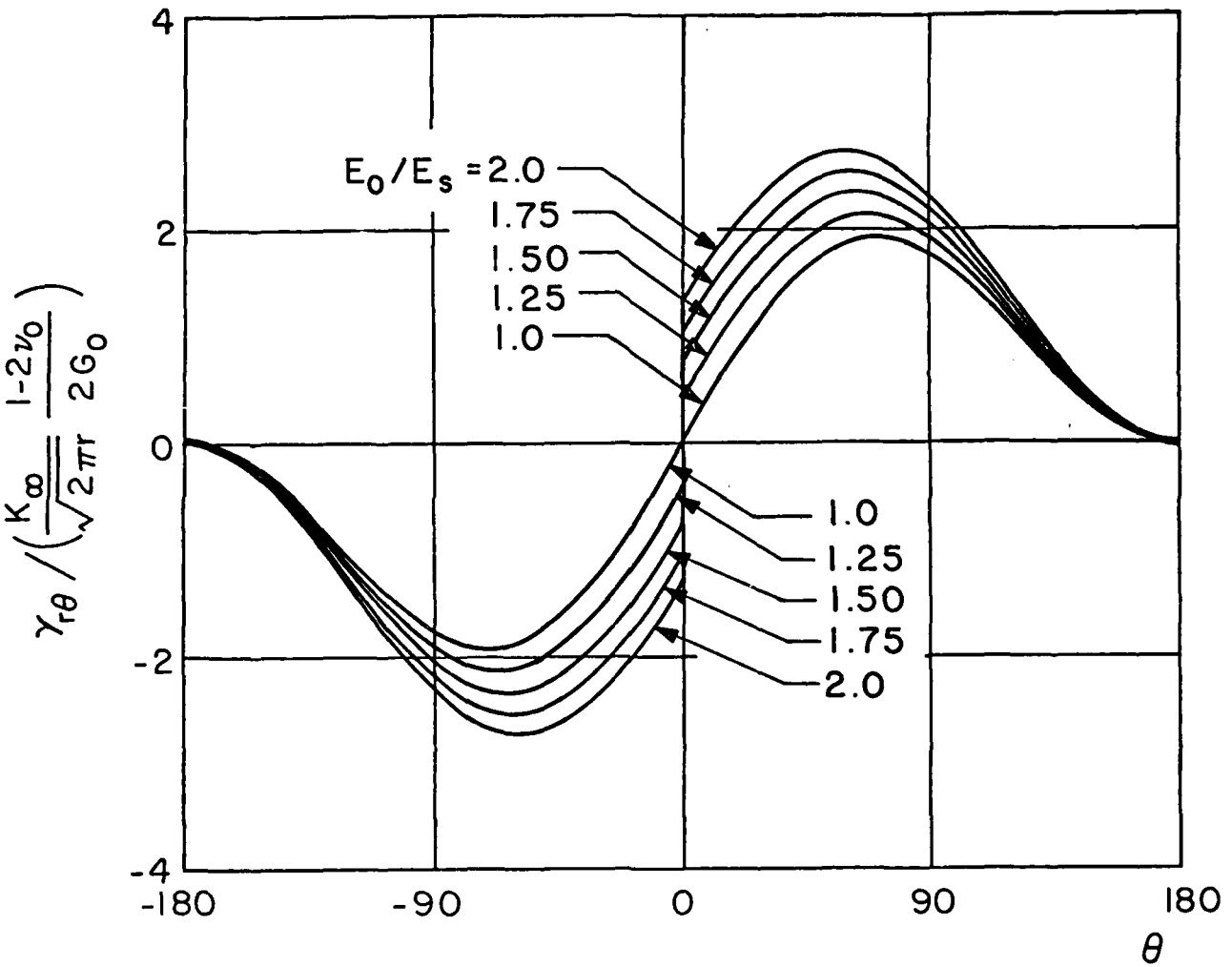
4
2
0
-2
-4
-180
-90
0
90
180
θ
$\gamma_{r\theta} / \left(\frac{K_\infty}{\sqrt{2\pi r}} \frac{1-2\nu_0}{2G_0}\right)$
E_0/E_s = 2.0
1.75
1.50
1.25
1.0
1.0
1.25
1.50
1.75
2.0

FIG. 3c

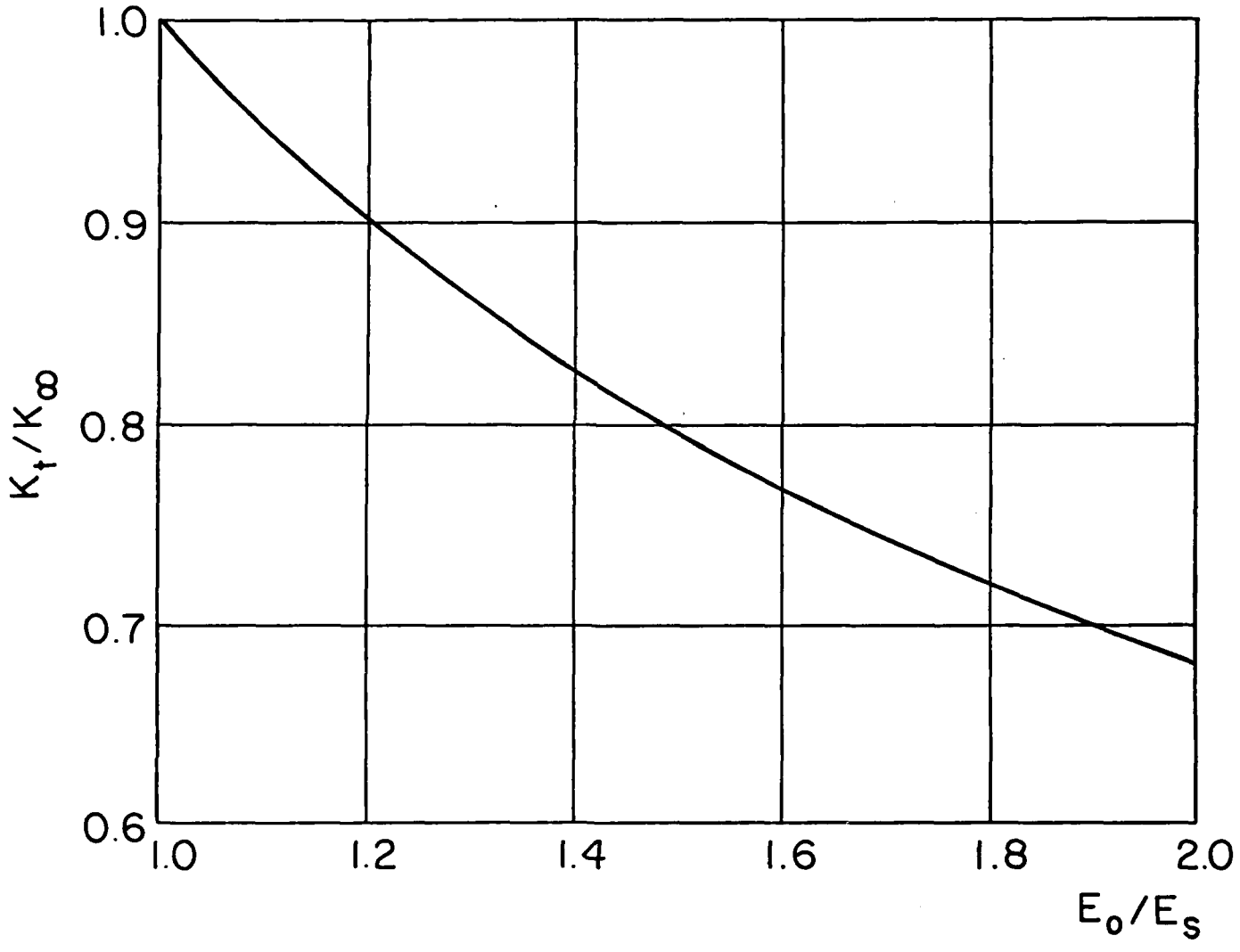

FIG. 4

END

DTIC

7-86